molecular pharmaceutics

Article

pubs.acs.org/molecularpharmaceutics

A Radiofluorinated Divalent Cystine Knot Peptide for Tumor PET Imaging

Lei Jiang,[†,‡,§] Richard H. Kimura,[‡,§] Xiaowei Ma,[‡] Yingfeng Tu,[‡] Zheng Miao,[‡] Bin Shen,[‡] Frederick T. Chin,[‡] Hongcheng Shi,[†] Sanjiv Sam Gambhir,[‡] and Zhen Cheng*[,‡]

[†]Department of Nuclear Medicine, Zhongshan Hospital, Fudan University, 180 Fenglin Road, Shanghai, China 200032

[‡]Molecular Imaging Program at Stanford (MIPS), Department of Radiology and Bio-X Program, Canary Center at Stanford for Cancer Early Detection, Stanford University, Stanford, California 94305, United States

Supporting Information

ABSTRACT: A divalent knottin containing two separate integrin binding epitopes (RGD) in the adjacent loops, 3-4A, was recently developed and reported in our previous publication. In the current study, 3-4A was radiofluorinated with a 4-nitrophenyl 2-^{18}F-fluoropropinate (^{18}F-NFP) group and the resulting divalent positron emission tomography (PET) probe, ^{18}F-FP−3-4A, was evaluated as a novel imaging probe to detect integrin $\alpha v\beta 3$ positive tumors in living animals. Knottin 3-4A was synthesized by solid phase peptide synthesis, folded, and site-specifically conjugated with $^{18/19}$F-NFP to produce the fluorinated peptide $^{18/19}$F-fluoropropinate-3-4A ($^{18/19}$F-FP−3-4A). The stability of ^{18}F-FP−3-4A was tested in both phosphate buffered saline (PBS) buffer and mouse serum. Cell uptake assays of the radiolabeled peptides were performed using U87MG cells. In addition, small animal PET imaging and biodistribution studies of ^{18}F-FP−3-4A were performed in U87MG tumor-bearing mice. The receptor targeting specificity of the radiolabeled peptide was also verified by coinjecting the probe with a blocking peptide cyclo(RGDyK). Our study showed that ^{18}F-FP−3-4A exhibited excellent stability in PBS buffer (pH 7.4) and mouse serum. Small animal PET imaging and biodistribution data revealed that ^{18}F-FP−3-4A exhibited rapid and good tumor uptake (3.76 ± 0.59% ID/g and 2.22 ± 0.62% ID/g at 0.5 and 1 h, respectively). ^{18}F-FP−3-4A was rapidly cleared from the normal tissues, resulting in excellent tumor-to-normal tissue contrasts. For example, liver uptake was only 0.39 ± 0.07% ID/g and the tumor to liver ratio was 5.69 at 1 h p.i. Furthermore, coinjection of cyclo(RGDyK) with ^{18}F-FP−3-4A significantly inhibited tumor uptake (0.41 ± 0.12 vs 1.02 ± 0.19% ID/g at 2.5 h) in U87MG xenograft models, demonstrating specific accumulation of the probe in the tumor. In summary, the divalent probe ^{18}F-FP−3-4A is characterized by rapid and high tumor uptake and excellent tumor-to-normal tissue ratios. ^{18}F-FP−3-4A is a highly promising knottin based PET probe for translating into clinical imaging of tumor angiogenesis.

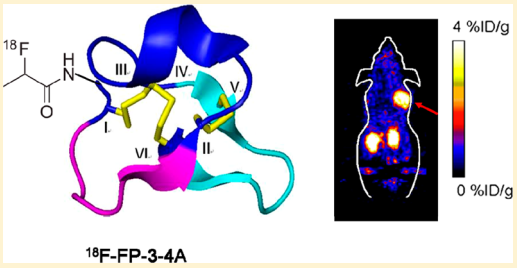

KEYWORDS: *cystine-knot peptide, divalent, integrin $\alpha_v\beta_3$, ^{18}F, PET*

INTRODUCTION

Members of the integrin family play important roles in the regulation of cellular activation, migration, proliferation, differentiation, and survival. Integrin receptors, including $\alpha v\beta 3$, $\alpha v\beta 5$, $\alpha v\beta 6$, and $\alpha 5\beta 1$, have been found to be highly expressed on many different cancer cells (glioblastomas, breast cancer, prostate cancer, melanomas, pancreas cancer, and so on), as well as on tumor neovasculature.[1−4] In particular, integrin $\alpha v\beta 3$ has been an attractive target for multimodal molecular imaging of tumors using a variety of imaging modalities, such as positron emission tomography (PET), single photon emission computed tomography (SPECT), optical imaging, ultrasound, magnetic resonance imaging (MRI) and so on.[5−7] Over the past several years, significant advances have been made in the development of molecular probes for imaging integrin expressing tumors. Numerous small peptide-based probes containing the arginine-glycine-aspartic acid (RGD) tripeptide motif such as cyclo(RGDyK) have been successfully developed for detection of integrin $\alpha v\beta 3$ *in vivo*.[8−14] Cystine knot peptides (also known as knottins) are small polypeptides that are characterized by a stable core motif formed by 3 disulfide bonds that are interwoven into a knotted conformation.[15,16] As a result, knottins have high thermal and proteolytic stability. In addition, the relatively small size (30−50 amino acids) makes them accessible by standard solid-phase peptide synthesis techniques. More importantly, knottins demonstrate fast blood clearance, high and specific tumor targeting ability, and biocompatibility, highlighting their potential use for patient imaging.[11,12] In our previous studies, monovalent integrin $\alpha v\beta 3$ knottin binders 2.5D, 2.5F, and

Special Issue: Positron Emission Tomography: State of the Art

Received: January 8, 2014
Revised: March 25, 2014
Accepted: April 9, 2014
Published: April 9, 2014

Table 1. Amino Acid Sequences of Ecballium Elaterium Trypsin Inhibitor (EETI) Mutants 2.5D, 2.5F, and 3-4A[a]

Knottin Peptide	Amino Acid Sequence	U87MG IC50 (nM)
2.5D	GCPQG**RGD**WAPTSCSQDSDCLAGCVCGPNGFCG	19±6
2.5F	GCPRP**RGD**NPPLTCSQDSDCLAGCVCGPNGFCG	26±5
3-4A	GCPQG**RGD**WAPTSCSQDSDCLAGCVCREA**RGD**MPRTCG	5±2

[a]IC50 was cited from refs 22 and 23. Black lines represent the disulfide bonds between Cys^1 and Cys^4, Cys^2 and Cys^5, and Cys^3 and Cys^6.

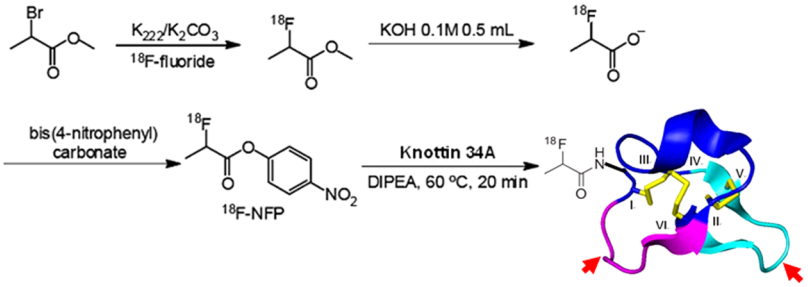

Figure 1. Schematic of knottin 3-4A. Yellow lines represent disulfide bonds between cystines (I–VI). Dark blue loop and light blue loop (red arrows indicate the purple and light blue loops containing RGD sequences) are engineered to contain an RGD motif, respectively. The imaging label ^{18}F-NFP was conjugated to the N-terminus of the knottin.

AgRP-7C (see sequences in Table 1) were labeled with a variety of reporting moieties (radionuclides and/or fluorescent dyes) and successfully used for multimodal imaging of tumors in small animal models.[17−23] The findings of these initial studies demonstrate that engineered knottins are promising for imaging of tumor targets such as integrin $\alpha v\beta 3$ *in vivo*.

Recently, divalent integrin $\alpha v\beta 3$ knottin binders including 3-4A (Figure 1; Table 1) were developed and reported in our previous publication.[18] The divalent knottins contain two separate integrin binding epitopes in adjacent loops (Table 1) and demonstrate improved integrin $\alpha v\beta 3$ binding affinity comparing to monovalent knottins.[18] In our current study, the divalent knottin 3-4A was site-specifically radiofluorinated by conjugating the N-terminus amino group of 3-4A with 4-nitrophenyl 2-^{18}F-fluoropropinate (^{18}F-NFP). The resulting PET probe, ^{18}F-FP−3-4A, was further evaluated *in vitro* and *in vivo* for their integrin $\alpha v\beta 3$ imaging properties using high integrin expressing glioblastoma U87MG cells and xenograft-bearing mice. Our study demonstrates that ^{18}F-FP−3-4A has good tumor uptake, low normal tissue accumulation, and high tumor-to-normal tissue ratios, which suggest that ^{18}F-FP−3-4A is the best performer among all the ^{18}F-labeled knottins developed so far.

MATERIALS AND METHODS

General. All 9-fluorenylmethyloxycarbonyl (Fmoc) protected amino acids were purchased from Novabiochem/EMD Chemicals Inc. (La Jolla, CA) or CS Bio (Menlo Park, CA). Phosphate buffered saline (PBS, 0.01 M, pH 7.4) was obtained from Gibco/Invitrogen (Carlsbad, CA). All other chemicals were purchased from Fisher Scientific (Fair Lawn, NJ) unless otherwise specified. The U87MG human glioblastoma cell line was obtained from American Type Culture Collection (Manassas, VA). Female athymic nude mice (nu/nu) were purchased from Charles River Laboratory (Wilmington, MA).

Preparative reversed-phase high performance liquid chromatography (RP-HPLC) using a Phenomenex Luna C18 column (5 μm, 250 × 10 mm) was performed on a Dionex 680 chromatography system with a UVD 170U absorbance detector and model 105S single channel radiation detector (Carroll & Ramsey Associates, Berkeley, CA). The recorded data were processed with use of Chromeleon version 6.50 software (Sunnyvale, CA). With a flow rate of 5.0 mL/min, the mobile phase was changed from 95% solvent A (10% acetonitrile/0.1% trifluoroacetic acid [TFA] in water) and 5% solvent B (0.1% TFA in acetonitrile [MeCN]) to 50% solvent A and 50% solvent B over 32 min. Analytical HPLC had a flow rate of 1.0 mL/min with a Phenomenex column (5 μm, 250 × 4.6 mm). The mobile phase was changed from 85% solvent A (10% water/0.1% trifluoroacetic acid [TFA] in water) and 15% solvent B (0.1% TFA in acetonitrile [MeCN]) to 35% solvent A and 65% solvent B over 26 min. Absorbance was monitored at 218 nm, and peptide identification was based on the UV spectrum acquired using a photodiode array (PDA) detector. All instruments, including matrix-assisted laser desorption/ionization time-of-flight mass spectrometry (MALDI-TOF-MS) instruments, RP-HPLC equipment including a radioaction detector, and a PET dose calibrator, were the same as those described previously.[22]

Chemistry and Radiochemistry. The linear knottin 3-4A (amino acid sequence shown in Table 1) was synthesized with a CS BioCS336 instrument using Fmoc-based solid-phase peptide synthesis, and the crude peptide was deprotected and cleaved from resin as reported previously.[18] Without intermediate purification, precursor peptide was oxidized and folded in 4 M guanidinium chloride, 10 mM reduced glutathione, 2

mM oxidized glutathione, and 3.5% (v/v) dimethyl sulfoxide (DMSO) at pH 8.0 in ammonium bicarbonate buffer at room temperature for 3 days with gentle mixing. Folded peptide was purified on a Vydac C18 preparatory scale column to 95% purity and lyophilized.

The synthesis of 4-nitrophenyl 2-fluoropropionate (^{19}F-NFP) conjugated 3-4A (^{19}F-FP−3-4A) is described as follows: 1 mg of bis-(4-nitrophenyl) carbonate (Sigma Chemical Company) was dissolved in 20 μL of *N*,*N*-dimethylformamide (DMF) as solution 1, next 2-fluoropropionic acid (FP, 2 μL) and 2 μL of *N*,*N*-diisopropylethylamine (DIPEA) were mixed as solution 2. Then solutions 1 and 2 were mixed together and incubated for 30 min at room temperature to prepare the ^{19}F-NFP. Lastly, 0.5 mg of 3-4A was dissolved in 20 μL of DMF and the solution mixed with ^{19}F-NFP overnight at room temperature. The resulting conjugate, ^{19}F-FP−3-4A, was purified by semipreparative RP-HPLC, and the fractions containing the product were collected and lyophilized. The identity of ^{19}F-FP−3-4A was confirmed by MALDI-TOF-MS.

^{18}F-NFP was prepared and used for 3-4A radiolabeling according to a previously reported protocol.[21] ^{18}F-NFP (specific activity of 40−100 GBq/μmol, at the end of synthesis in 200 μL of DMSO) and 40 μL of DIPEA were added to 400 μg of 3-4A peptide and reacted for 20 min at 60 °C. After addition of 1 mL of 95% water/5% acetic acid to quench the reaction, the radiolabeled product was separated by semi-preparative HPLC using the same elution gradient. The HPLC fractions containing ^{18}F-FP−3-4A were collected and dried with a rotary evaporator. The radiolabeled peptide was reconstituted in PBS and passed through a 0.22 μm Millipore filter into a sterile vial for *in vitro* and *in vivo* experiments.

Cell Culture and Animal Model. U87MG cells were cultured in Dulbecco's modified Eagle's high-glucose medium (GIBCO, Carlsbad, CA) and supplemented with 10% fetal bovine serum (FBS) and 1% penicillin−streptomycin in a humidified incubator containing 5% CO_2 at 37 °C. A 70−80% confluent monolayer was detached with 0.25% trypsin-ethylenediaminetetraacetic acid (EDTA) and dissociated into a single-cell suspension for further cell culture and assays.

All animal studies were carried out in compliance with federal and local institutional rules for the conduct of animal experimentation. Approximately 1×10^7 cultured U87MG cells were suspended in 100 μL of PBS and subcutaneously implanted in the right shoulders of nude mice. Tumors were grown to a size of 0.5−1 cm in diameter (2−3 weeks).

***In Vitro* Stability.** ^{18}F-FP−3-4A (3.7−5.55 MBq [100−150 μCi]) was incubated in 0.5 mL of mouse serum for 1 h at 37 °C. The mixture was then treated with 0.5 mL of acetonitrile to precipitate the serum protein and centrifuged at 16000*g* for 2 min. The supernatant containing greater than 95% of the radioactivity was filtered using a 0.22 μm nylon SpinX column (Corning Inc.). Greater than 99% of the radioactivity passed through this filter. In addition, ^{18}F-FP−3-4A (3.7−5.55 MBq [100−150 μCi]) was also incubated in PBS buffer for 1 h at room temperature. The samples were analyzed by radio-HPLC. The high sensitive Bioscan detector and low sensitivity Ramsey detector were used for analysis of mouse serum stability sample and PBS sample, respectively. The percentage of intact peptide was determined by quantifying peaks corresponding to the intact peptide and degradation products.[17]

U87MG Cell Uptake Assay. Cell uptake studies were performed as previously described.[17] Briefly, U87MG cells (1×10^5) were seeded in 12-well tissue culture plates and allowed to attach overnight. After the wash with 0.01 M PBS for 3 times, the cells were incubated with ^{18}F-FP−3-4A (37 kBq, 1 μCi per well, in culture medium) with or without the blocking peptide, c(RGDyK) (2 μg/well, an unlabeled integrin-binding peptide), at 37 °C for different time points, including 15 min, 30 min, 60 min, and 120 min. The cells were then washed 3 times with PBS and lysed in 0.5 mL of 1.0 M NaOH. Radioactivity was measured by using a γ-counter (PerkinElmer 1470, Waltham, MA). Cell uptake was expressed as the percentage of added radioactivity. Experiments were performed twice with triplicate wells.

Small Animal PET Imaging. PET imaging of tumor-bearing mice was performed using a small animal PET scanner (Siemens Inveon). Mice bearing U87MG (n = 4 for each group) xenografts were injected via the tail vein with approximately 3.7 MBq (100 μCi) of ^{18}F-FP−3-4A with or without ∼330 μg of c(RGDyK). At 0.5, 1, and 2 h postinjection (p.i.), mice were anesthetized with 2% isoflurane (5% for induction and 2% for maintenance in 100% O_2) for imaging experiments. The images were reconstructed with the two-dimensional ordered-subset expectation maximization (OSEM 2D) algorithm. The method for quantification analysis of small animal PET images was the same as previously reported.[15]

Biodistribution Studies. U87MG tumor-bearing mice (n = 4 for each group) were injected with approximately 1.85−3.7 MBq (50−100 μCi) of ^{18}F-FP−3-4A via the tail vein and sacrificed at different time points from 0.5 to 2.5 h p.i. Tumor and normal tissues of interest were removed and weighed, and their radioactivity levels were measured with a γ-counter. The radioactivity uptake in the tumor and normal tissues was expressed as a percentage of the injected radioactive dose per gram of tissue (% ID/g). To test the $\alpha v\beta 3$ integrin-targeting specificity of ^{18}F-FP−3-4A *in vivo*, U87MG tumor-bearing mice (n = 4 for each group) were injected via the tail vein with a mixture of the probe 1.85−3.7 MBq (50−100 μCi) of ^{18}F-FP−3-4A and 330 μg of c(RGDyK). The mice were sacrificed, and biodistribution of ^{18}F-FP−3-4A at 2.5 h after injection was determined.

Statistical Analysis. The quantitative data were expressed as mean ± SD. Means were compared using the Student t test. A 95% confidence level was chosen to determine the significance between groups, with P values of less than 0.05 indicating significant differences.

RESULTS

Chemistry and Radiochemistry. Knottin 3-4A was synthesized by solid phase peptide synthesis, folded *in vitro*, and purified by RP-HPLC. ^{19}F-FP−3-4A was prepared by site-specific conjugation of ^{19}F-NFP to the N terminus of 3-4A with a 92% yield. This nonradioactive compound was used as a standard for radiosynthesis and integrin receptor binding assays. Chemical purity of ^{19}F-FP−3-4A was greater than 95%, as determined by analytical HPLC. Molecular masses of the products were determined by MALDI-TOF-MS. Folded peptide 3-4A recorded an m/z value of 3938.2, which corresponded to the $[MH]^+$ (calculated m/z = 3938.6). For ^{19}F-FP−3-4A, the recorded m/z value was 4012.3 for $[MH]^+$ (calculated m/z = 4012.6). The retention times on the analytical HPLC for folded 3-4A and ^{19}F-FP−3-4A were 10.3 and 13.3 min, respectively.

Radiosynthesis of ^{18}F-NFP was completed in approximately 100 min using a modified GE synthetic module (TRACERlab FXFN). The coupling of ^{18}F-NFP and 3-4A was achieved in

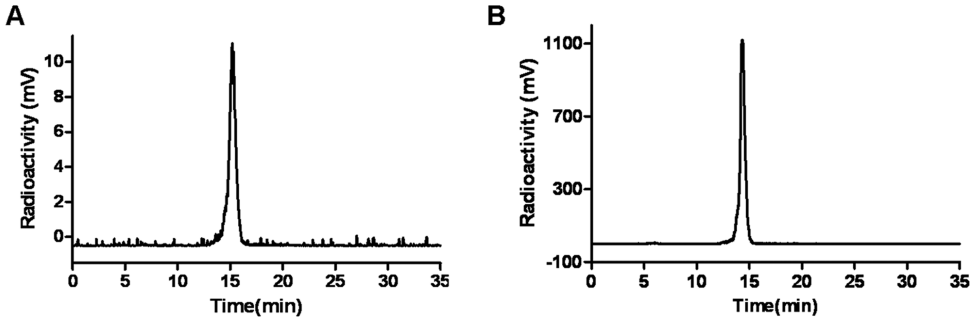

Figure 2. Stability analysis of ^{18}F-FP−3-4A in PBS buffer and mouse serum. The probe was incubated with PBS buffer for 1 h at room temperature (A) or mouse serum for 1 h at 37 °C (B).

decay-corrected yields of 5−10%. Because the unlabeled 3-4A could be easily separated from the ^{18}F-FP−3-4A, the radiochemical purity of ^{18}F-FP−3-4A was found to be > 90% as determined by HPLC, and the specific radioactivity of the probe was estimated to be >37 GBq/μmol using the prosthetic labeling agent ^{18}F-NFP as a reference standard.

Peptide Stability. ^{18}F-FP−3-4A was completely intact after 1 h in 0.01 M PBS (pH 7.4), as determined by radio-HPLC analysis (Figure 2A). More importantly, radio-HPLC analysis also revealed that over 95% of the probe remained intact after 1 h incubation in mouse serum at 37 °C (Figure 2B).

***In Vitro* Cell Uptake Assay.** Cellular uptake of ^{18}F-FP−3-4A was evaluated using U87MG cells, and the results are shown in Figure 3. During the first 15 min incubation period at both 4 and 37 °C, ^{18}F-FP−3-4A exhibited rapid initial accumulation in the cells followed by a steady increase in receptor mediated uptake throughout the experiment. However, compared to 4 °C, binding to cell surface receptors and subsequent internalization were much greater at 37 °C. The cell uptake values of ^{18}F-FP−3-4A at 15, 30, 60, and 120 min at 37 °C were 0.71 ± 0.07%, 0.90 ± 0.04%, 1.44 ± 0.04%, and 1.50 ± 0.07%, respectively, while at 4 °C values of 0.32 ± 0.02%, 0.41 ± 0.11%, 0.44 ± 0.05%, and 0.51 ± 0.04% were observed, respectively (Figure 3). A 2−3-fold greater accumulation of the probe occurred in cells incubated at 37 °C compared to those incubated at 4 °C, which is indicative of internalization that occurs at physiological temperature. Moreover, cell surface binding and internalization could be significantly inhibited by the presence of a large excess of c(RGDyK) ($P < 0.05$). As shown in Figure 3, cells of the blocking groups at 37 and 4 °C displayed minimal uptake. At 1 h, cell uptake of the probe was inhibited 70.14% and 31.82% at 37 and 4 °C, respectively, suggesting that the probe was specifically binding to integrin $\alpha v\beta 3$.

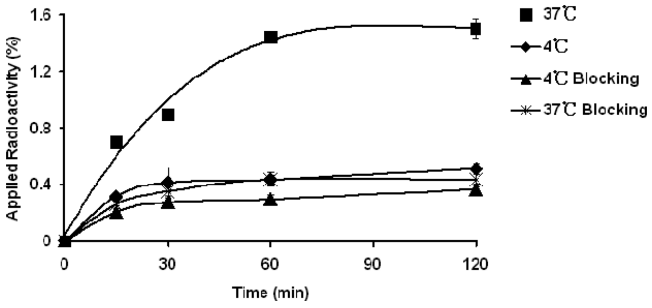

Figure 3. *In vitro* cell binding and uptake assay. U87MG cells were incubated with 37 kBq (1 μCi) for various time points at 4 or 37 °C, with or without addition of 2 μg of c(RGDyK). Data represents mean percentage of total radioactivity added, measured in triplicate, and error bars represent SD.

Small Animal PET Imaging Studies. Representative coronal and transverse small-animal PET images of U87MG tumor-bearing mice ($n = 4$) at different time points (0.5, 1, and 2 h) after injection are shown in Figure 4A. The tumors were clearly visible at 0.5 h after injection and demonstrated high contrast with low contralateral background from 0.5 to 1 h, which persisted to 2 h after injection. Relatively high kidney uptake was observed at early time points and beyond, again indicating a renal clearance route. Most of the nontargeted organs demonstrated relatively low signal, indicating low accumulation of the probe. Further quantification analysis showed that the tumor uptake was 3.87 ± 0.66% ID/g at 0.5 h p.i., whereas normal tissues such as lung, liver, heart, and muscle exhibited much lower uptakes than the tumor (Figure 4B).

Coinjection of excess c(RGDyK) was used as a blocking agent. Significantly reduced tumor uptake of ^{18}F-FP−3-4A was observed (3.87 ± 0.66% ID/g vs 0.60 ± 0.06% ID/g at 0.5 h p.i.) (Figure 4A and C), which confirmed specific targeting of the probe to integrin $\alpha v\beta 3$ receptor. In addition, no visible bone uptake was observed, suggesting no observable defluorination of the probe *in vivo* within 2 h p.i.

Biodistribution Studies. The biodistribution of ^{18}F-FP−3-4A was examined in nude mice bearing U87MG human glioblastoma tumors, and the results are shown in Table 2. Tumor uptake of the probe was 3.76 ± 0.59, 2.22 ± 0.62, and 1.02 ± 0.19% ID/g at 0.5, 1, and 2.5 h, respectively, indicating the high tumor uptake and moderate tumor retention rate of the probe. ^{18}F-FP−3-4A displayed rapid blood clearance, and the radioactive level remaining in the blood at 0.5 and 2.5 h p.i. was measured to be 0.64 ± 0.07 and 0.29 ± 0.09% ID/g, respectively. Moreover, whole-body clearance of radioactivity was rapid. Except for the kidneys, accumulations in most of normal organs examined were lower than 1% ID/g at 1 h p.i. Especially, the liver uptake was only 0.68 ± 0.12% ID/g at 0.5 h p.i. Relatively high uptake was observed in the kidneys at early time points (6.98 ± 1.61% ID/g at 0.5 h), and quickly decreased to 1.10 ± 0.22% ID/g at 2.5 h p.i. These data clearly indicate a renal excretion route and metabolic processing of the probe mainly by the kidneys. With the rapid clearance of the probe from blood and other normal organs, it was found that ^{18}F-FP−3-4A exhibited high U87MG tumor-to-normal organ (blood, muscle, lung, liver, spleen, pancreas, etc.) ratios (Table 2). At 0.5 h p.i., the tumor-to-blood, tumor-to-muscle, and

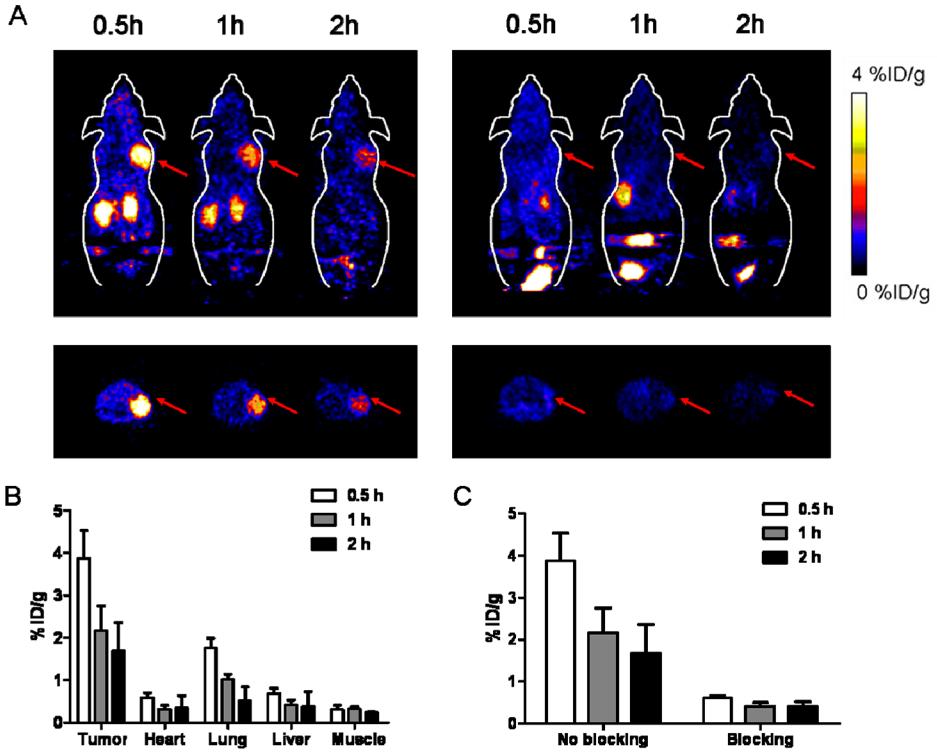

Figure 4. Small animal PET images and quantification analysis results. (A) Representative coronal (top row) and transverse (bottom row) small-animal PET imaging of U87MG tumor-bearing mice at 0.5, 1, and 2 h after injection of 1.85−3.7 MBq (50−100 μCi) of ^{18}F-FP−3-4A with (right images) or without (left images) coinjection of ~330 μg of cyclo(RGDyK). (B) Quantification analysis of radioactivity accumulation in selected organs at different time points after injection of ^{18}F-FP−3-4A, reported as % ID/g. (C) Quantification analysis of radioactivity accumulation of probe in tumor with or without coinjection of cyclo(RGDyK) at 0.5, 1, and 2 h after injection.

Table 2. Biodistribution Results for ^{18}F-FP−3-4A in Nude Mice Bearing Subcutaneously Xenotransplanted U87MG Human Glioblastoma[a]

	^{18}F-FP−3-4A			^{18}F-FP−3-4A + c(RGDyK)
organ	0.5 h	1 h	2.5 h	2.5 h
% ID/g				
tumor	3.76 ± 0.59	2.22 ± 0.62	1.02 ± 0.19	0.41 ± 0.12*
blood	0.64 ± 0.07	0.36 ± 0.07	0.29 ± 0.09	0.30 ± 0.09
heart	0.48 ± 0.08	0.30 ± 0.06	0.29 ± 0.05	0.21 ± 0.02
lungs	1.73 ± 0.27	0.94 ± 0.08	0.54 ± 0.10	0.47 ± 0.18
liver	0.68 ± 0.12	0.39 ± 0.07	0.29 ± 0.10	0.19 ± 0.04
spleen	0.88 ± 0.06	0.47 ± 0.04	0.48 ± 0.10	0.24 ± 0.05*
stomach	1.81 ± 0.08	1.07 ± 0.02	0.68 ± 0.16	0.29 ± 0.12*
pancreas	0.32 ± 0.13	0.22 ± 0.02	0.21 ± 0.08	0.19 ± 0.03
intestine	1.28 ± 0.32	0.94 ± 0.05	0.48 ± 0.09	0.28 ± 0.08*
kidneys	6.98 ± 1.61	3.02 ± 0.33	1.10 ± 0.22	1.94 ± 0.75
brain	0.13 ± 0.03	0.09 ± 0.00	0.15 ± 0.06	0.09 ± 0.01
skin	1.30 ± 0.08	0.68 ± 0.05	0.40 ± 0.10	0.27 ± 0.01
muscle	0.35 ± 0.10	0.22 ± 0.05	0.25 ± 0.04	0.16 ± 0.06
bone	0.79 ± 0.17	0.48 ± 0.21	0.20 ± 0.17	0.37 ± 0.25
ratio				
tumor-to-blood	5.94 ± 0.94	4.39 ± 0.82	3.12 ± 0.55	1.36 ± 0.15
tumor-to-muscle	10.80 ± 1.52	10.09 ± 1.22	3.47 ± 0.07	2.85 ± 1.46
tumor-to-lung	2.22 ± 0.45	1.44 ± 0.31	1.64 ± 0.01	0.90 ± 0.20
tumor-to-liver	5.55 ± 0.63	5.69 ± 0.88	3.15 ± 0.74	2.10 ± 0.22
tumor-to-spleen	4.28 ± 0.40	2.63 ± 0.32	1.83 ± 0.16	1.69 ± 0.12
tumor-to-pancreas	11.98 ± 1.94	6.06 ± 0.54	3.96 ± 1.24	1.96 ± 0.60
tumor-to-kidney	0.57 ± 0.19	0.60 ± 0.12	0.72 ± 0.15	0.19 ± 0.02

[a]*P < 0.05, compared with ^{18}F-FP−3-4A data at 2.5 h. Data are presented as % ID/g tissue ± SD (n = 4) after intravenous injection of the probe (1.85−3.7 MBq, [50−100 μCi]) at 0.5, 1, and 2.5 h (n = 4). For 2.5 h blocking group, mice were coinjected with ~330 μg of cyclo(RGDyK).

dx.doi.org/10.1021/mp500018s | *Mol. Pharmaceutics* 2014, 11, 3885−3892

Table 3. Comparison of ^{18}F Labeled Probes for Imaging Integrin $\alpha v\beta 3$ Targeted Tumor[a]

probes	U87MG IC50[b] (nm)	biodistribution data at 1 h					ref
		tumor	liver	kidney	tumor-to-liver ratio	tumor-to-muscle ratio	
^{18}F-FP−3-4A	5 ± 2[c]	2.22 ± 0.62	0.39 ± 0.07	3.02 ± 0.33	5.69	10.09	
^{18}F-FP−2.5D	7.4 ± 1.9	2.86 ± 1.11	∼1.2	4.24 ± 1.94	∼2.38	∼4.3	17
^{18}F-FP−2.5F	7.5 ± 1.3	3.60 ± 0.25	∼2.5	5.25 ± 0.65	∼1.44	∼4	17
^{18}F-FP−AgRP-7C	∼8.37	2.39 ± 0.15	∼0.5	∼20	∼4.78	∼7	20
^{18}F-FP−PRGD2	51.8 ± 4.6	2.80 ± 0.46	0.63 ± 0.09	2.88 ± 0.42	∼4.44	∼9.03	25
^{18}F-AlF−NOTA-RGD2	46 ± 4.4	5.3 ± 1.7	∼3	4.24 ± 1.94	∼2.38	∼4.3	28

[a]The xenotransplanted tumor model was nude mice with U87MG human glioblastoma. [b]The IC50 values of integrin $\alpha v\beta 3$-targeting radiotracers were measured with 3-4A, ^{19}F-FP−2.5D,^{19}F-FP−2.5F,^{19}F-FP−AgRP-7C,^{19}F-FP−PRGD$_2$ and ^{19}F-AlF−NOTA-RGD$_2$. [c]The affinity of ^{19}F-FP−3-4A is shown in Supporting Information Figure 1.

tumor-to-liver ratios of ^{18}F-FP−3-4A were 5.94, 10.80, and 5.55, respectively.

In vivo tumor targeting specificity of ^{18}F-FP−3-4A was then evaluated by coinjection of the probe with a large amount of c(RGDyK). It was found that coinjection with c(RGDyK) significantly reduced tumor uptake of the probe by ∼60% of the corresponding control tumor uptake (1.02 ± 0.19% ID/g vs 0.41 ± 0.12% ID/g, $P < 0.05$) (Table 2). Interestingly significant differences were also found for some other normal tissues between the blocking group and the control group, and these tissues include the stomach, intestine, and spleen.

DISCUSSION

The development of new PET probes allows quantification of cancer-specific cell surface receptors and detection of tumors. Several laboratories including ours have explored grafting and directed evolution strategies to develop imaging probes based on highly structured protein scaffolds or molecular frameworks that could be engineered to bind cancer markers. In this regard, cystine-knot peptides are emerging as very promising scaffolds for molecular imaging because they can be engineered to bind tumor biomarkers with high affinity and specificity. Recently, several studies reported the development of engineered knottin mutants from Agouti related protein (AgRP, four disulfide bonds) and *Ecballium elaterium* trypsin inhibitor (EETI-II, three disulfide bonds), which can bind to integrin $\alpha v\beta 3$ receptors with low nanomolar affinities.[15,16,22] In addition, the relatively small size and multiple disulfide-bonded structure of knottin peptides generally lead to excellent proteolytic resistance and thermal stability, fast *in vivo* clearance from normal organs and rapid tumor accumulation. Knottin peptides can also be chemically synthesized and tolerate significant modifications to their N-terminus with different labeling moieties without sacrificing target binding properties.[15,16]

In the current study, the selection of ^{18}F as a radiolabel is based on (1) its wide availability and great potential for clinical translation; (2) the ideal physical properties of ^{18}F ($t_{1/2}$: 110 min, emits 635 keV β^+ particles, 99% abundant) for PET imaging; (3) the physical half-life of ^{18}F complements the rapid blood clearance of knottin peptides. ^{18}F-NFP was selected as a prosthetic group for site-specific radiofluorination of the knottin because of its small size, high *in vivo* stability, and well-established production method.[21,24−26] Our studies showed that divalent knottin 3-4A could easily be radiolabeled with ^{18}F-NFP. *In vitro* stability assays indicated that ^{18}F-FP−3-4A was very stable in mouse serum.[27]

In vitro U87MG cell uptake assays showed that ^{18}F-FP−3-4A exhibited good cell uptake and receptor-mediated internalization at 37 °C, which is evident by the higher uptake values of the probe at 37 °C compared to those at 4 °C (Figure 3). Moreover, around 70% of the cell uptake of ^{18}F-FP−3-4A can be blocked by coincubation with an excess of unlabeled c(RGDyK) at 37 °C, suggesting that the probe specifically binds integrins $\alpha v\beta 3$. Collectively, these results further warrant the biological evaluation of ^{18}F-FP−3-4A in *in vivo* experiments.

In vivo biodistribution and small animal PET imaging studies revealed that the EETI-II based divalent probe, ^{18}F-FP−3-4A, had favorable tumor-targeting properties, including rapid and high tumor uptake, fast clearance from blood and most normal tissues, and high tumor-to-normal tissue ratios. This probe showed very low uptake in liver (0.68, 0.39, and 0.29% ID/g at 0.5, 1, and 2.5 h p.i.) (Table 2). In our previous studies, the monovalent engineered EETI-II knottins 2.5D and 2.5F (with one RGD motif) were radiolabeled with ^{18}F-NFP, and the resulting probes, ^{18}F-FP−2.5D and ^{18}F-FP−2.5F, were also evaluated in nude mice bearing U87MG tumor xenografts.[21] As shown in Table 3, compared with ^{18}F-FP−2.5D and ^{18}F-FP−2.5F, ^{18}F-FP−3-4A showed much higher tumor-to-normal tissues ratio, such as tumor-to-muscle (10.09 vs. 4.3 and 4) and tumor-to-liver (5.69 vs. 2.38 and 1.44) at 1 h p.i. These data clearly suggest the advantages of using divalent probe ^{18}F-FP−3-4A for imaging of lesions in liver. Moreover, the renal uptake of ^{18}F-FP−3-4A is lower than that of ^{18}F-FP−2.5D and ^{18}F-FP−2.5F. The improved imaging results of this probe could be partially due to its higher binding affinity compared to other knottin binders (Table 1). It also should be noted that knottin 3-4A has good binding selectivity as it showed high binding affinity to integrins $\alpha v\beta 3$ and $\alpha v\beta 5$ and lower affinity for $\alpha 5\beta 1$ and αiib$\beta 3$.[22] Interestingly, our previous study showed that the AgRP scaffold based knottin PET probe, ^{18}F-FP−AgRP-7C, displayed very low uptake in liver (∼0.5% ID/g at 1 h), but extremely high uptake in kidney (∼20% ID/g at 1 h p.i.) (Table 3).[20] ^{18}F-FP−3-4A circumvents the relatively high liver uptake of monovalent EETI-II knottins (2.5D and 2.5F) probe and high kidney uptake of the AgRP probe (AgRP-7C), while maintaining the good tumor uptake and retention properties. To date, ^{18}F-FP−3-4A demonstrates superior performance over other integrin avb3 binding knottins tested in living animals. Due to improved performance in the liver, this probe may be well suited for molecular imaging of liver metastasis or liver fibrosis.[28]

The integrin $\alpha v\beta 3$ receptor has also been widely imaged by a series of radiofluorinated monomeric, dimeric, and tetrameric RGD peptide-based PET probes.[29−31] At present, many of the monomeric, dimeric, and tetrameric RGD peptides have been commercially available and are much easier to obtain. Among

them, ^{18}F-FP−PRGD$_2$ is a very promising agent and has been evaluated in clinical studies. Compared to the biodistribution data of ^{18}F-FP−PRGD$_2$, ^{18}F-FP−3-4A displayed similar tumor uptake (2.22 ± 0.62 vs 2.80 ± 0.46 at 1 h p.i.), but slightly lower liver accumulation (0.39 ± 0.07 vs 0.63 ± 0.09 at 1 h p.i.) and thus higher tumor-to-liver ratio (∼5.69 vs ∼4.44) (Table 3).[31] Recently, ^{18}F-AlF−NOTA-RGD$_2$ was also prepared through a one-step radiosynthesis procedure and showed thus a higher U87MG tumor uptake of 5.7 ± 2.1 and 5.3 ± 1.7% ID/g at 0.5 and 1 h, respectively.[32] However, liver uptake of ^{18}F-AlF−NOTA-RGD$_2$ was also quite high (∼3% ID/g at both 0.5 and 1 h, respectively) (Table 3). The tumor-to-liver and tumor-to-muscle ratios of ^{18}F-AlF−NOTA-RGD$_2$ were significantly lower than those of ^{18}F-FP−3-4A (∼2.38 vs 5.69 and ∼4.3 vs 10.09 at 1 h p.i.). Therefore, compared to these small cyclic dimeric RGD based probes, ^{18}F-FP−3-4A may provide better image quality and better biodistribution profiles.

CONCLUSIONS

Divalent knottin 3-4A was successfully radiolabeled with ^{18}F-NFP for imaging integrin $\alpha v\beta 3$ positive U87MG tumor in living animals. ^{18}F-FP−3-4A showed integrin-specific PET imaging of U87MG tumors marked by fast and good tumor accumulation, rapid clearance from blood and other normal tissues, and high tumor-to-normal tissue ratios, such as tumor to liver ratio. These results indicate that ^{18}F-FP−3-4A is a promising imaging probe and has the potential to translate to the application in clinic.

ASSOCIATED CONTENT

Supporting Information

Additional figure showing the binding affinity of 3-4A and ^{19}F-FP−3-4A and additional experimental details. This material is available free of charge via the Internet at http://pubs.acs.org.

AUTHOR INFORMATION

Corresponding Author

*Molecular Imaging Program at Stanford, Department of Radiology and Bio-X Program, Canary Center at Stanford for Cancer Early Detection, 1201 Welch Road, Lucas Expansion, P095, Stanford University, Stanford, CA 94305-5484. Tel: 650-723-7866. Fax: 650-736-7925. E-mail: zcheng@stanford.edu.

Author Contributions

§L.J. and R.H.K. contributed equally to the work.

Notes

The authors declare no competing financial interest.

ACKNOWLEDGMENTS

This work was supported, in part, by the Office of Science (BER), U.S. Department of Energy (DE-SC0008397), NCI In Vivo Cellular Molecular Imaging Center (ICMIC) Grant P50 CA114747, National Science Foundation for Young Scholars of China (Grant No. 81101072), and Foundation of Zhongshan Hospital for Youth Scholars (Grant No. 2012ZSQN03).

ABBREVIATIONS USED

PET, positron emission tomography; SPECT, single photon emission computed tomography; HPLC, high-performance liquid chromatography; % ID/g, % injected radioactive dose per gram of tissue; p.i., postinjection

REFERENCES

(1) Hynes, R. O. Integrins: versatility, modulation, and signaling in cell adhesion. *Cell* **1992**, *69* (1), 11−25.

(2) Brooks, P. C.; Clark, R. A.; Cheresh, D. A. Requirement of vascular integrin alpha v beta 3 for angiogenesis. *Science* **1994**, *264* (5158), 569−71.

(3) Seftor, R. E.; Seftor, E. A.; Gehlsen, K. R.; Stetler-Stevenson, W. G.; Brown, P. D.; Ruoslahti, E.; Hendrix, M. J. Role of the alpha v beta 3 integrin in human melanoma cell invasion. *Proc. Natl. Acad. Sci. U.S.A.* **1992**, *89* (5), 1557−61.

(4) Streuli, C. H.; Akhtar, N. Signal co-operation between integrins and other receptor systems. *Biochem. J.* **2009**, *418* (3), 491−506.

(5) Cai, W.; Rao, J.; Gambhir, S. S.; Chen, X. How molecular imaging is speeding up antiangiogenic drug development. *Mol. Cancer Ther* **2006**, *5* (11), 2624−33.

(6) Cai, W.; Chen, X. Multimodality molecular imaging of tumor angiogenesis. *J. Nucl. Med.* **2008**, *49* (Suppl.2), 113S−28S.

(7) Beer, A. J.; Schwaiger, M. Imaging of integrin alphavbeta3 expression. *Cancer Metastasis Rev.* **2008**, *27* (4), 631−44.

(8) Ruoslahti, E. RGD and other recognition sequences for integrins. *Annu. Rev. Cell Dev. Biol.* **1996**, *12*, 697−715.

(9) Cheng, Z.; Wu, Y.; Xiong, Z.; Gambhir, S. S.; Chen, X. Near-infrared fluorescent RGD peptides for optical imaging of integrin alphavbeta3 expression in living mice. *Bioconjugate Chem.* **2005**, *16* (6), 1433−41.

(10) Liu, S. Radiolabeled cyclic RGD peptides as integrin alpha(v)beta(3)-targeted radiotracers: maximizing binding affinity via bivalency. *Bioconjugate Chem.* **2009**, *20* (12), 2199−213.

(11) Liu, Z.; Shi, J.; Jia, B.; Yu, Z.; Liu, Y.; Zhao, H.; Li, F.; Tian, J.; Chen, X.; Liu, S.; Wang, F. Two (9)(0)Y-labeled multimeric RGD peptides RGD4 and 3PRGD2 for integrin targeted radionuclide therapy. *Mol. Pharmaceutics* **2011**, *8* (2), 591−9.

(12) Liu, Z.; Jia, B.; Shi, J.; Jin, X.; Zhao, H.; Li, F.; Liu, S.; Wang, F. Tumor Uptake of the RGD Dimeric Probe (99m)Tc-G3−2P4-RGD2 is Correlated with Integrin alphavbeta3 Expressed on both Tumor Cells and Neovasculature. *Bioconjugate Chem.* **2010**, *21* (3), 548−55.

(13) Haubner, R.; Kuhnast, B.; Mang, C.; Weber, W. A.; Kessler, H.; Wester, H. J.; Schwaiger, M. [18F]Galacto-RGD: synthesis, radiolabeling, metabolic stability, and radiation dose estimates. *Bioconjugate Chem.* **2004**, *15* (1), 61−9.

(14) Liu, Z.; Liu, S.; Wang, F.; Chen, X. Noninvasive imaging of tumor integrin expression using (18)F-labeled RGD dimer peptide with PEG (4) linkers. *Eur. J. Nucl. Med. Mol. Imaging* **2009**, *36* (8), 1296−307.

(15) Silverman, A. P.; Levin, A. M.; Lahti, J. L.; Cochran, J. R. Engineered cystine-knot peptides that bind alpha(v)beta(3) integrin with antibody-like affinities. *J. Mol. Biol.* **2009**, *385* (4), 1064−75.

(16) Kimura, R. H.; Levin, A. M.; Cochran, F. V.; Cochran, J. R. Engineered cystine knot peptides that bind alphavbeta3, alphavbeta5, and alpha5beta1 integrins with low-nanomolar affinity. *Proteins* **2009**, *77* (2), 359−69.

(17) Jiang, L.; Miao, Z.; Kimura, R. H.; Silverman, A. P.; Ren, G.; Liu, H.; Lu, H.; Cochran, J. R.; Cheng, Z. 111In-labeled cystine-knot peptides based on the Agouti-related protein for targeting tumor angiogenesis. *J. Biomed. Biotechnol.* **2012**, *2012*, 368075.

(18) Jiang, L.; Miao, Z.; Kimura, R. H.; Liu, H.; Cochran, J. R.; Culter, C. S.; Bao, A.; Li, P.; Cheng, Z. Preliminary evaluation of (177)Lu-labeled knottin peptides for integrin receptor-targeted radionuclide therapy. *Eur. J. Nucl. Med. Mol. Imaging* **2011**, *38* (4), 613−22.

(19) Jiang, L.; Kimura, R. H.; Miao, Z.; Silverman, A. P.; Ren, G.; Liu, H.; Li, P.; Gambhir, S. S.; Cochran, J. R.; Cheng, Z. Evaluation of a (64)Cu-labeled cystine-knot peptide based on agouti-related protein for PET of tumors expressing alphavbeta3 integrin. *J. Nucl. Med.* **2010**, *51* (2), 251−8.

(20) Miao, Z.; Ren, G.; Liu, H.; Kimura, R. H.; Jiang, L.; Cochran, J. R.; Gambhir, S. S.; Cheng, Z. An engineered knottin peptide labeled with 18F for PET imaging of integrin expression. *Bioconjugate Chem.* **2009**, *20* (12), 2342−7.

(21) Liu, S.; Liu, H.; Ren, G.; Kimura, R. H.; Cochran, J. R.; Cheng, Z. PET Imaging of Integrin Positive Tumors Using F Labeled Knottin Peptides. *Theranostics* **2011**, *1*, 403−12.
(22) Kimura, R. H.; Jones, D. S.; Jiang, L.; Miao, Z.; Cheng, Z.; Cochran, J. R. Functional mutation of multiple solvent-exposed loops in the Ecballium elaterium trypsin inhibitor-II cystine knot miniprotein. *PLoS One* **2011**, *6* (2), e16112.
(23) Kimura, R. H.; Cheng, Z.; Gambhir, S. S.; Cochran, J. R. Engineered knottin peptides: a new class of agents for imaging integrin expression in living subjects. *Cancer Res.* **2009**, *69* (6), 2435−42.
(24) Jiang, H.; Moore, S. J.; Liu, S.; Liu, H.; Miao, Z.; Cochran, F. V.; Liu, Y.; Tian, M.; Cochran, J. R.; Zhang, H.; Cheng, Z. A novel radiofluorinated agouti-related protein for tumor angiogenesis imaging. *Amino Acids* **2013**, *44* (2), 673−81.
(25) Chin, F. T.; Shen, B.; Liu, S.; Berganos, R. A.; Chang, E.; Mittra, E.; Chen, X.; Gambhir, S. S. First experience with clinical-grade ([18F]FPP(RGD(2)): an automated multi-step radiosynthesis for clinical PET studies. *Mol. Imaging Biol.* **2012**, *14* (1), 88−95.
(26) Liu, H.; Liu, S.; Miao, Z.; Jiang, H.; Deng, Z.; Hong, X.; Cheng, Z. A Novel Aliphatic ^{18}F-Labeled Probe for PET Imaging of Melanoma. *Mol. Pharmaceutics* **2013**, *10* (9), 3384−91.
(27) G, C. The anachronisms of pictures. *Science* **1886**, *7* (163), 264.
(28) Li, F.; Song, Z.; Li, Q.; Wu, J.; Wang, J.; Xie, C.; Tu, C.; Huang, X.; Lu, W. Molecular imaging of hepatic stellate cell activity by visualization of hepatic integrin alphavbeta3 expression with SPECT in rat. *Hepatology* **2011**, *54* (3), 1020−30.
(29) Cai, W.; Zhang, X.; Wu, Y.; Chen, X. A thiol-reactive 18F-labeling agent, N-[2-(4−18F-fluorobenzamido)ethyl]maleimide, and synthesis of RGD peptide-based tracer for PET imaging of alpha v beta 3 integrin expression. *J. Nucl. Med.* **2006**, *47* (7), 1172−80.
(30) Wu, Z.; Li, Z. B.; Cai, W.; He, L.; Chin, F. T.; Li, F.; Chen, X. 18F-labeled mini-PEG spacered RGD dimer (18F-FPRGD2): synthesis and microPET imaging of alphavbeta3 integrin expression. *Eur. J. Nucl. Med. Mol. Imaging* **2007**, *34* (11), 1823−31.
(31) Liu, S.; Liu, Z.; Chen, K.; Yan, Y.; Watzlowik, P.; Wester, H. J.; Chin, F. T.; Chen, X. 18F-labeled galacto and PEGylated RGD dimers for PET imaging of alphavbeta3 integrin expression. *Mol. Imaging Biol.* **2010**, *12* (5), 530−8.
(32) Liu, S.; Liu, H.; Jiang, H.; Xu, Y.; Zhang, H.; Cheng, Z. One-step radiosynthesis of (1)(8)F-AlF-NOTA-RGD(2) for tumor angiogenesis PET imaging. *Eur. J. Nucl. Med. Mol. Imaging* **2011**, *38* (9), 1732−41.